Erschienen in: 35th European Photovoltaic Solar Energy Conference and Exhibition / Verlinden, Pierre et al. (Hrsg.). - München : WIP, 2018. - S. 342-345. - ISBN 978-3-936338-50-8

INFLUENCE OF LOW-TEMPERATURE ANNEALING BEFORE FIRING ON LETID IN MULTICRYSTALLINE SILICON

Andreas Schmid, Jeanette Lindroos, Annika Zuschlag, Daniel Skorka, Jakob Fritz, Giso Hahn
University of Konstanz, Department of Physics, 78457 Konstanz, Germany

ABSTRACT: Light and elevated temperature induced degradation (LeTID) affects significantly the performance of multicrystalline silicon (mc-Si) solar cells. Even though the underlying mechanisms of LeTID and subsequent regeneration are still unknown, LeTID formation is known to be influenced by surface passivation, firing, and low-temperature annealing after firing. Since both the firing peak temperature and the cooling profile strongly influence LeTID, firing is presumed to dominate over any preceding low-temperature steps. However, lifetime measurements during illumination (1.0 ±0.1 suns) at 150°C show a clear difference in the LeTID defect density in samples annealed at 200-500°C *before* aluminum oxide deposition and *before* firing. Additionally, LeTID becomes worse when the pre-firing annealing is performed in an H plasma atmosphere. Therefore, the firing step does not erase the impact of low-temperature annealing or pre-firing hydrogenation on LeTID. Finally, thinner samples are shown to cause lower initial effective lifetimes (τ_{eff}) and less LeTID.

Keywords: Degradation, Multicrystalline Silicon, Annealing, Lifetime, Hydrogen, LeTID

1 INTRODUCTION

Multicrystalline (mc) Si PERC (passivated emitter and rear cell) solar cells, but also lifetime samples, show a strong degradation under illumination at elevated temperatures (*e.g.* [1-4]), known as light and elevated temperature induced degradation (LeTID). Previously known degradation mechanisms, such as the dissociation of FeB pairs and BO defects, cannot explain the observed degradation kinetics [1-3]. After degradation, solar cells [3] as well as lifetime samples [5] show a regeneration, but the underlying mechanisms of both effects are still unknown. However, the kinetics of both degradation and regeneration are known to be influenced by material properties, e.g. sample thickness [6], and treatment conditions, such as illumination and temperature (*e.g.* [3, 7]). Additionally, a low temperature dark annealing step *after* firing is known to impact LeTID formation in mc-Si [8]. However, as LeTID only forms at firing temperatures above 675°C [9], the firing step is presumed to dominate over any preceding low temperature steps. Interestingly, the surface passivation layer has been shown to also influence the LeTID defect density [10]. Passivation layers were deposited with different PECVD (plasma-enhanced chemical vapor deposition) tools, and it is still unknown whether the deposition temperature plays a role in LeTID formation. In this contribution, we subject sister wafers to different low temperature annealing steps (T_{var}< 500°C) in N_2 atmosphere *before* firing, after which we deposit the same Al_2O_3 layer on all samples.

Capture cross section analysis of the LeTID defect has hinted at a metal impurity [11, 12], whereas the impact of the PECVD passivation layer and the wafer thickness (*e.g.* [12-15]) indicate a direct involvement of hydrogen in the LeTID mechanism. Hence, we additionally apply an H plasma atmosphere during the low-temperature annealing step to investigate the influence of hydrogen on degradation and regeneration.

2 EXPERIMENTAL

To investigate the influence of a low temperature step before firing on LeTID and regeneration behavior, high quality B-doped p-type mc-Si sister wafers with comparable grain and defect structure from the middle of the ingot were processed to lifetime samples (5 x 5 cm^2). To further investigate the influence of sample thickness, half of the wafers were etched to a thickness of 150 µm, the rest to 170 µm. A scheme of the applied process sequence is given in Fig. 1. Half of the wafers were gettered via $POCl_3$ diffusion (55 Ω/□), after which the emitter was removed. Next, all samples were deposited with thin PECVD SiO_x at room temperature to protect the samples from contamination during low temperature annealing. The samples were annealed for different times (0.5-2 h) in a tube furnace at different temperatures (T_{var} <500°C).

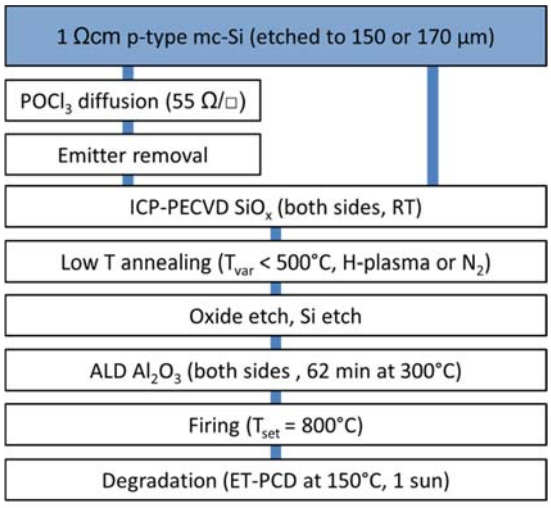

Figure 1: Process sequence of the investigated lifetime samples.

To investigate the influence of hydrogen on LeTID and regeneration behavior, half of the wafers were annealed in H plasma atmosphere, which was realized by microwave-induced remote hydrogen plasma (MIRHP). The rest of the wafers were annealed in N_2 atmosphere. After SiO_x and silicon etching, all samples were deposited with double-sided 30 nm Al_2O_3 at 300°C by atomic layer deposition (ALD) for a total of 62 min. Finally, all samples were fired in a belt furnace at a set temperature of 800°C.

Konstanzer Online-Publikations-System (KOPS)
URL: http://nbn-resolving.de/urn:nbn:de:bsz:352-2-1qn9mmicwi29b6

For degradation, lifetime samples were held at a temperature of approx. 150°C under illumination with halogen lamps (1.0 ±0.1 suns). The effective minority charge carrier lifetime τ_{eff} was measured repetitively with photoconductance decay (PCD) at elevated temperature (ET) of 150°C. The lifetime was extracted at a fixed excess charge carrier concentration of $\Delta n = 1.5 \times 10^{15}$ cm^{-3}. Additionally, spatially resolved lifetime maps were measured at certain stages of degradation and regeneration (after firing, at the degraded state and after full regeneration) with the self-calibrated TR-PLI method [16] at room temperature (RT).

3 RESULTS

In the following either gettered or ungettered sample sets are shown and discussed. Nevertheless, all the observed results match qualitatively in each case.

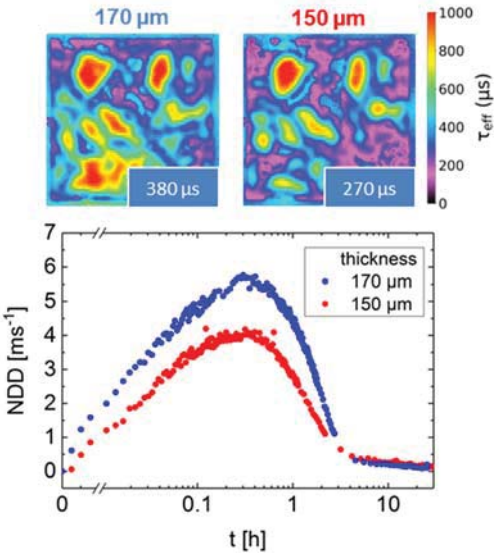

Figure 2: TR-PLI lifetime maps with harmonic average τ_{eff} values before degradation of two ungettered sister samples with the thickness of 150 and 170 µm, respectively, annealed in N_2 atmosphere at 400°C for 30 min (top). Normalized defect density (NDD) of these two samples (150°C, 1 sun) calculated from the extracted ET-PCD lifetimes (bottom).

3.1 Influence of sample thickness

TR-PLI lifetime maps of two ungettered sister wafers with the thicknesses of 150 and 170 µm, respectively, are shown in Fig. 2. Fig. 2 also shows the time-dependent normalized defect density (NDD), which is calculated using

$$\mathrm{NDD}(t) = \frac{1}{\tau_{\mathrm{eff}}(t)} - \frac{1}{\tau_{\mathrm{eff}}(0)} \quad (1)$$

where $\tau_{\mathrm{eff}}(t)$ and $\tau_{\mathrm{eff}}(0)$ are the extracted effective lifetimes measured with ET-PCD at any given time and the initial state, respectively. Both samples received a low temperature annealing step at 400°C in N_2 atmosphere before ALD Al_2O_3 passivation and firing. The thicker sample (170 µm) shows an initial harmonic average τ_{eff} of 380 µs, the thinner sample (150 µm) only 270 µs.

Regarding NDD, both samples show pronounced LeTID and a following regeneration phase. While the thicker sample shows stronger degradation, both samples regenerate completely to their starting values within a few hours. These observations are less pronounced but match qualitatively with [6], which also shows an influence of the sample thickness on LeTID and regeneration. In the model discussed in [6], a movement of impurities towards the wafer surface is assumed to be responsible for regeneration.

3.2 Low-temperature annealing before firing

To investigate the influence of a low temperature annealing step before firing, Fig. 3 shows the initial TR-PLI lifetime images of six gettered sister samples before degradation. The reference sample was only subjected to Al_2O_3 passivation before firing, whereas the other samples were annealed at 200, 300 and 400°C for 0.5-2 h before ALD and firing.

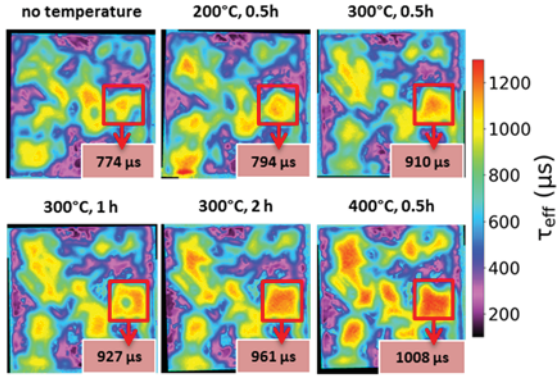

Figure 3: Initial TR-PLI lifetime maps (before illumination) of gettered sister samples subjected to different low temperature annealing steps in N_2 atmosphere before ALD and firing. The red squares highlight the change of one sample area with increasing temperature and annealing time. The harmonic average τ_{eff} values of this area are shown in the lower right corner.

It can be seen that a low temperature annealing step before firing improves initial τ_{eff}. As highlighted by the red squares in Fig. 3, adding a low temperature step of 200°C improves the lifetime from 774 to 794 µs. Elevating the temperature further to 400°C increases the lifetime up to 1008 µs. At 300°C, extending the annealing time from 30 min to 2 h increases τ_{eff} again from 910 to 961 µs. All of these improvements in the initial lifetime might be caused by low temperature gettering of impurities internally or towards the surface layer during the low-temperature annealing steps.

Fig. 4 displays the normalized defect density of the discussed samples. Within approx. 10 min of illumination, all the low temperature annealed samples have reached full degradation, but with significantly different defect densities. The reference sample without an additional low temperature annealing step shows weak LeTID, which remains at a similar level even when a 30 min anneal at 300°C is added before ALD and firing. Interestingly, extending the annealing time to 1 h at 300°C leads to the highest NDD. Regardless of the annealing temperature, LeTID becomes stronger by extending the step from 30 min to 1 h.

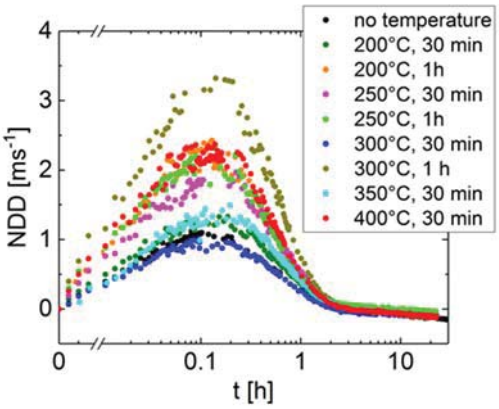

Figure 4: Normalized defect density of gettered sister samples annealed in N_2 atmosphere at 200-400°C for 0.5 and 1 h before Al_2O_3 deposition and firing.

While there is no obvious correlation between the temperature and the LeTID kinetics, the low temperature annealing before surface passivation and firing changes the maximum LeTID defect density reached in the degradation/regeneration cycle. This means that the LeTID precursor/s is/are very sensitive to even small temperature variations below 500°C, and the effects of this temperature load is not erased by the following firing step.

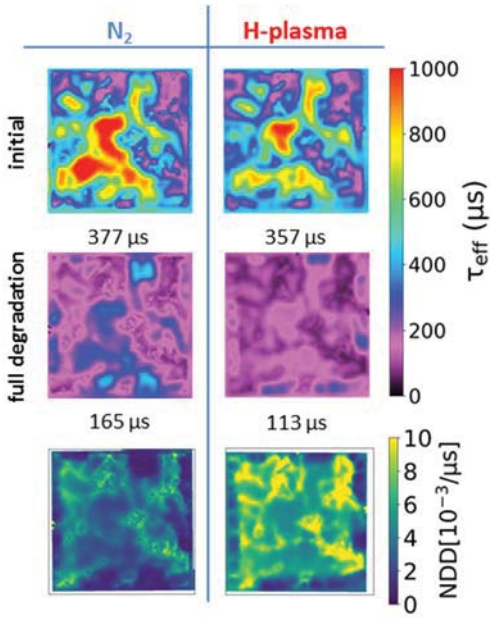

Figure 5: TR-PLI lifetime maps at initial state and after full degradation of two ungettered sister samples. Both samples underwent an annealing step at 300°C for 30 min but in different atmospheres (left column: N_2, right column: H plasma). The last row shows the NDD maps, calculated according to Eq. 1 with the respective lifetime maps above.

3.3 Influence of hydrogen

Fig. 5 shows the initial TR-PLI lifetime maps (directly after firing and after full degradation) of two ungettered sister wafers, which underwent an annealing step at 300°C for 30 min. The left sample was annealed in N_2 atmosphere, whereas remote hydrogen plasma was present during the annealing of the sample shown on the right. Comparing the lifetime maps at the initial state, the harmonic average τ_{eff} is clearly reduced from 377 to 357 µs by the presence of H plasma before ALD Al_2O_3 passivation. The spatially resolved maps reveal that areas with high τ_{eff} are decreasing, whereas areas with low τ_{eff} increase during H plasma annealing. This reduction in areas with high τ_{eff} is a first indication of the detrimental effect of pre-firing hydrogenation, which was already discussed in [15] and could lead to an issue regarding high performance mc-Si. The TR-PLI lifetime maps after full degradation shows that the sample treated in H plasma and therefore most probably containing more H in the Si bulk is affected more by LeTID, which was also recently observed in [17]. To further quantify these observations, the lifetime maps after firing and after full degradation were aligned to each other and NDD of each pixel was calculated according to Eq. 1. The resulting NDD maps are shown in the bottom row of Fig. 5. It can be seen that the sample with H-plasma present during annealing suffer much more from LeTID than the sample annealed in N_2 atmosphere.

Furthermore, a comparison of the NDD map with the initial TR-PLI lifetime map shows that areas with low initial τ_{eff} are more affected, but this is the case in both investigated samples. To further confirm these observations, time dependent NDD was calculated with ET-PCD data and is shown in Fig. 6.

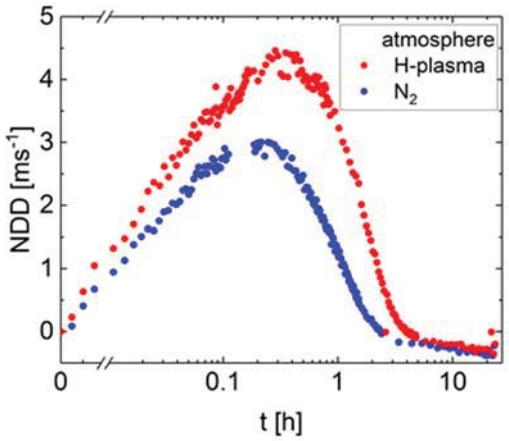

Figure 6: Normalized defect density calculated with ET-PCD data of the two sister samples displayed in Fig. 5.

A comparison of the differently treated samples shows clearly the detrimental impact of hydrogen on LeTID. The maximum NDD is significantly higher for the sample treated in H-plasma atmosphere. Additionally, a time shift of several minutes in reaching maximum NDD is visible. Interestingly, both samples regenerate completely. Whereas the sample annealed in N_2 atmosphere regenerates after approx. 2 h, the sample treated in H plasma atmosphere reaches the initial lifetime after 3 h. This might be due to the time shift in reaching maximum NDD.

This effect is not limited to the samples annealed at 300°C. All samples subjected to pre-firing annealing show higher LeTID in either the spatially resolved NDD maps measured at room temperature or the NDD plots calculated with ET-PCD data, when the annealing is performed in H plasma. The annealing step only influences the strength of this effect, which might be caused by a strong dependency on the local defect structure or a strong sensitivity to small experimental variations (*e.g.*, temperature ramps during

unloading of samples after low temperature annealing). Note that PCD data only show weighted average values of part of the sample and the extracted data can be misinterpreted. So when trying to evaluate measurements of mc-Si samples, a combination of spatially resolved measurements (*cf*. Fig. 5) and PCD measurements (*cf*. Fig. 6) is necessary and seems to be a good solution.

4 SUMMARY AND DISCUSSION

The influence of sample thickness, low temperature annealing *before* firing, and the effect of an H plasma on LeTID and regeneration could be shown on mc-Si wafers using data from TR-PLI and ET-PCD. Spatially resolved τ_{eff} was combined with injection dependent τ_{eff} for detailed analysis of the effect of annealing and sample thinning. The effect of sample thickness on LeTID and regeneration which was already discussed in [6] could be confirmed, and its influence on initial τ_{eff} could additionally be demonstrated with spatially resolved lifetime maps.

A comparison of samples that underwent a low temperature anneal at 200-500°C for 0.5-2 h *before* surface passivation and firing showed an initial lifetime increase, which might be caused by low temperature gettering internally or towards the surface layer. The different annealing profiles clearly influenced the maximum defect density, but no obvious relation was found between the chosen temperature and the LeTID kinetics. Therefore, the LeTID precursor/s is/are observed to be very sensitive to even small temperature variations below 500°C *before* firing, and the effects of these steps are not erased by the following firing step.

In addition, we could show the combined detrimental and beneficial influence on the initial τ_{eff} of hydrogen introduced before ALD AlO_x surface passivation and firing. TR-PLI and ET-PCD measurements enabled a detailed comparison regarding LeTID and regeneration behavior of samples either annealed in N_2 or in H plasma atmosphere. While pre-firing hydrogen worsens LeTID, all samples regenerate to their initial τ_{eff} value after a few hours at 150°C. These results help explain why the surface passivation deposition step itself affects LeTID, and ultimately why LeTID varies so much in mc Si-PERC solar cells from different manufacturers.

5 ACKNOWLEDGEMENTS

Part of this work was supported by the German BMWi under contracts 0324204B, 0325763B and 0324001. The content of the publication is the responsibility of the authors. The authors would like to thank L. Mahlstaedt, B. Rettenmaier and J. Engelhardt for technical support.

6 REFERENCES

[1] K. Ramspeck, S. Zimmermann, H. Nagel, A. Metz, Y. Gassenbauer, B. Birkmann, A. Seidl, Proc. 27th EUPVSEC, Frankfurt/Main, Germany, 2012, 861.
[2] F. Fertig, K. Krauss, S. Rein, Physica Status Solidi RRL 9(1) (2014) 41.
[3] F. Kersten, P. Engelhart, H.-C. Ploigt, A. Stekolnikov, T. Lindner, F. Stenzel, M. Bartzsch, A. Szpeth, K. Petter, J. Heitmann, J. Müller, Solar Energy Materials and Solar Cells 142 (2015) 83.
[4] A. Zuschlag, D. Skorka, G. Hahn, Progress in Photovoltaics: Research and Applications 25(7) (2017) 545.
[5] A. Zuschlag, D. Skorka, G. Hahn, Proc. 43rd IEEE PVSC, Portland 2016, 1051.
[6] D. Bredemeier, D.C. Walter, J. Schmidt, Solar RRL 2 (2018) 1700159.
[7] J. Fritz, A. Zuschlag, D. Skorka, G. Hahn, Energy Procedia 124 (2017) 718.
[8] C.E. Chan, T.H. Fung, M.D. Abbott, D. Payne, A. Wellham, B. Hallam, R. Chen, S. Wenham, Solar RRL 1 (2017) 1600028.
[9] C.E. Chan, D.R. Payne, B.J. Hallam, M.D. Abbott, T.H. Fung, A.M. Wenham, B.S. Tjahjono, S.R. Wenham, IEEE Journal of Photovoltaics 6 (2016) 1473.
[10] F. Kersten, J. Heitmann, J.W. Müller, Energy Procedia 92 (2016) 828.
[11] A.E. Morishige, M.A. Jensen, D.B. Needleman, K. Nakayashiki, J. Hofstetter, T.-T.A. Li, T. Buonassisi, IEEE Journal of Photovoltaics 6(6) (2016) 1466.
[12] K. Nakayashiki, J. Hofstetter, A. Morishige, T. Li, D. Needleman, M. Jensen, T. Buonassisi, IEEE Journal of Photovoltaics 6(4) (2016) 860.
[13] T.H. Fung, M. Kim, D. Chen, C.E. Chan, B.J. Hallam, R. Chen, D.N.R. Payne, A. Ciesla, S.R. Wenham, M.D. Abbott, Sol. En. Mat. Sol. Cells 184 (2018) 48.
[14] D. Bredemeier, D.C. Walter, J. Schmidt, AIP Conference Proceedings 1999 (2018) 130001.
[15] D. Chen, P.G. Hamer, M. Kim, T.H. Fung, G. Bourret-Sicotte, S. Liu, C.E. Chan, A. Ciesla, R. Chen, M.D. Abbott, B.J. Hallam, S.R. Wenham, Solar Energy Materials and Solar Cells 185 (2018) 174.
[16] D. Kiliani, G. Micard, B. Steuer, B. Raabe, A. Herguth, G. Hahn, Journal of Applied Physics 110 (2011) 054508.
[17] M.A. Jensen, A. Zuschlag, D. Skorka, S. Wieghold, A.E. Morishige, G. Hahn, T. Buonassisi, Journal of Applied Physics 124(8) (2018) 085701.